

---

CHAPTER - VI

---

## S U M M A R Y   A N D   C O N C L U S I O N S

Ferrites constitute a class of important materials which have wide ranging applications in the field of electronics technology and in microwave devices. Recent researches have shown that it is possible to process ferrites having desired properties to suit the requirements of a particular application.

In the present work the studies on DC electrical conductivity and magnetization of Co-Zn ferrites are reported. Cobalt ferrites have many applications as device material in electronics and microwave devices. Many researchers have tried to improve their electrical, dielectric and magnetization properties. The saturation magnetization, one of the important parameters for application purpose, is quite high in Cobalt ferrites and is expected to be improved upon still further by the addition of Zinc. Co-Zn ferrites have been studied by quite a few workers. Jonker [1] has investigated the semiconducting properties of mixed crystals of Cobalt ferrites. Josyulu and Sobhanadri [2] and Satyanarayana [3] have studied the DC conductivity and dielectric properties of Co-Zn ferrites. Saturation moments of Co-Zn ferrites have been measured and studied by Guillaud et al [4]. The effect of sintering time on these electrical

and magnetic properties of Co-Zn ferrites have been very rarely studied.

In the present case observations on DC electrical conductivity and magnetization of Co-Zn ferrites sintered for two different sintering times have been reported and explained in the light of their microstructure obtained by using scanning electron microscopy.

The orientation of the problem thus involved the following studies on the Co-Zn  $\text{Fe}_2\text{O}_4$  system.

- (1) Preparation of the Co-Zn $\text{Fe}_2\text{O}_4$  ferrites with  $x = 0, 0.2, 0.4, 0.6, 0.8$  and  $1,$
- (2) Characterization of ferrites by XRD,
- (3) Measurement of DC electrical resistivity,
- (4) Measurement of magnetization, and IR absorption studies,
- (5) Calculation of porosity, study of microstructure obtained with SEM, and to establish correlation between microstructure and properties of ferrites.

Chapter I gives a brief account of historical developments, spinel structure, properties and applications of ferrites along with the orientation of the problem for the present work.

The preparation and characterization of ferrites is dealt with in chapter II. Methods of preparation of ferrite composition are discussed and the general ceramic method of

ferrite preparation is represented by a 'flow chart'. Co-Zn ferrites with the general formula  $\text{Co}_x\text{Zn}_{1-x}\text{Fe}_2\text{O}_4$  (with  $x = 0, 0.2, 0.4, 0.6, 0.8$  and  $1$ ) were prepared by the conventional double sintering process. Cobalt oxide, Zinc oxide and Ferric oxide (all AR grade) were mixed in stoichiometric proportions and presintered in air at  $800^\circ\text{C}$  for 20 hrs. By taking the presintered powder in a die and subjecting it to a hydraulic pressure of about 10 tons for 5 minutes, pellets each weighing 1 gm approximately and measuring 1 cm in diameter and 0.2 - 0.3 cm in thickness were prepared. These pellets were subjected to final sintering in a Silicon Carbide furnace. As it was desired to study the effect of sintering time on physical properties, one series of pellets was sintered at  $900^\circ\text{C}$  for 15 hrs, and the other at  $900^\circ\text{C}$  for 30 hrs.

X-ray diffraction patterns for all of our samples were obtained using Fe -  $K_\alpha$  radiation. XRD maxima were indexed by usual method and lattice parameter for each Co-Zn ferrite was calculated. All samples have exhibited cubic structure. The compositional variation of lattice parameter with Zn content in the sample obeys Vegard's law. The lattice parameter is minimum for  $\text{CoFe}_2\text{O}_4$ , increases linearly with the addition of Zn, and becomes maximum for  $\text{ZnFe}_2\text{O}_4$ . The

variation is explained on the basis of atomic volume differences of Co and Zn.

Bond lengths  $R_A$  and  $R_B$  for each sample were calculated using the relations

$$R_A = \sqrt{3} a \left[ \frac{1}{8} + \varepsilon \right]$$

and

$$R_B = a \sqrt{\frac{1}{16} - \frac{\varepsilon}{2} + 3\varepsilon^2}$$

where  $\varepsilon = u - 0.375$ , the deviation from oxygen parameter.

Bond length  $R_A$  increases linearly with the increase of Zn content in ferrite sample. This is considered to be associated with the increase of lattice parameter as Zn content in the sample increases.  $R_B$  decreases nonlinearly with increasing Zn content. This is attributed to the increase in ionocovalent character of bonding with the increasing Zn content in the sample [5].

The site radii  $r_A$  and  $r_B$  were calculated using relations

$$r_A = \sqrt{3} a \left[ u - \frac{1}{4} \right] - r(O^{2-}),$$

and 
$$r_B = a \left[ \frac{5}{8} - u \right] - r(O^{2-}),$$

where  $u$  = oxygen parameter of ferrite

and  $r(O^{2-})$  = Goldsmit radius of  $O^{2-}$

$$= 1.35 \text{ \AA}.$$

Site radius  $r_A$  increases linearly, and  $r_B$  decreases non-linearly with increasing Zn content in sample. Since  $r_A$  values calculated for our system  $\text{Co}_x\text{Zn}_{1-x}\text{Fe}_2\text{O}_4$  are much smaller than the ionic radii of  $\text{Co}^{2+}, \text{Zn}^{2+}, \text{Fe}^{3+}, \text{Fe}^{2+}$  ions, it is concluded that the site radii ( $r_A$ ) of A-sites are too small to admit these ions without local distortion of site or ion, or both [6].

In chapter III, the conduction models in ferrites and experimental measurement of electrical resistivity are discussed. The electrical resistivity was measured on  $\text{Co}_x\text{Zn}_{1-x}\text{Fe}_2\text{O}_4$  system between room temperature and  $700^\circ\text{C}$  by two probe method.

The plots of  $\log_{10} \rho$  vs  $\left[ \frac{10^3}{T} \right]$  are linear and show change in slope at temperatures which agree well with Curie temperatures of corresponding samples. The change in slope is attributed to the disordering of electron spins at the Curie temperature [7]. These breaks are supposed to suggest some predominant change in conduction mechanism due to magnetic phase transition. The break point on the curve separates upper ferrimagnetic region from lower paramagnetic region.

The activation energies in both the regions have been calculated from the slopes of the curves using the conductivity law in ferrites. The activation energy for paramagnetic region is greater than that for ferrimagnetic region. This shows that the magnetic ordering has a role in influencing conductivity. The lowering of activation energy is attributed to such an ordering [8]. Activation energies of our samples vary from 0.2 - 0.55 ev., and high activation energy is accompanied by low conductivity. Our results of activation energy are in agreement with the theory given by Irkhin and Turov [9]. For electron hopping the values of activation energies are reported to be 0.2ev or less [10,11]. As our activation energy values are greater than 0.2ev, conductivity may be due to the hopping of polarons. The increase of Cobalt concentration in the samples increases

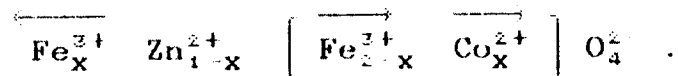
their conductivity. This is attributed to the presence of large number of Cobalt ions in the variable valency.

It has been observed that the activation energy and porosity of our samples decrease with increasing sintering time. Such results have been explained on the basis of microstructural changes brought in by sintering conditions. For higher sintering time as densification increases porosity decreases, and consequently the impending paths to electrons are reduced. This results in increase in conductivity of the sample.

Part-A of chapter IV is devoted for the theoretical background of magnetization in ferrites and the experimental study on magnetization of Co-Zn ferrites. High field loop tracer, supplied by Arun Electronics, Bombay was used to measure magnetization of the samples. It is observed that the saturation magnetization ( $M_S$ ) and magnetic moment ( $\mu_B$ ) increase to a maximum value when Zn-content in the sample is 40%. Beyond this composition  $M_S$  and  $\mu_B$  decrease slowly becoming almost zero for  $ZnFe_2O_4$ .



$Zn^{2+}$  is a non magnetic ion and has a strong preference for A-site, on going to A-site, it forces equal number of  $Fe^{3+}$  ions to B-site and the resultant cation distribution becomes



The magnetic moment of this formula unit is given by

$$\mu_B = 5(2-x) + mx - 5x,$$

where  $m = 3$  Bohr magnetons (for Cobalt). Thus on the basis of this formula the  $\mu_B$  should start from  $\mu_B = m = 3$  for pure Cobalt ferrite and should tend to 10 Bohr magnetons [12]. However, in practice this value of 10 is never realised. It is because Zn-ferrite is anti-ferromagnetic even in the mixed ferrimagnetic Zn-ferrite. The effect of this interaction is usually marked by the strong A-B interactions which cause the spins in B-site to be aligned parallel to each other. However, the substitution of Zn-ions on A-site weakens the A-B interaction, and when  $Zn^{2+}$  ions subsituated on A-site approach 40% to 50%, the B-B interaction becomes comparable in strength with A-B interaction, and magnetic moment decreases [13].

The cation distribution for all samples is calculated using Gilleo's formula.  $\mu_B$  values calculated from this cation distribution do not agree well with those experimentally observed for samples with Zn-content more than 40%. It is therefore concluded that Gilleo's formula is not applicable to evaluate cation distribution in  $\text{Co}_x\text{Zn}_{1-x}\text{Fe}_2\text{O}_4$  ferrite system beyond 40% Zn content in the sample [14].

$M_s$  and  $\mu_B$  are found to increase slightly with increase in sintering time. This rise in magnetization is explained on the basis of redistribution of cations with the increase in sintering time, and also on the basis of microstructural changes brought in during sintering.

At higher sintering time\temperature  $\text{Fe}^{3+}$  ions (with  $\mu = 5$ ) on A-site may diffuse to their preferred B-site and thus increasing the magnetic moment of B-site and hence the net magnetic moment of the ferrite sample.

Microstructure also plays an important role in increasing the magnetization at higher sintering time\temperature. Each grain possesses certain resultant magnetic moment. The increase in sintering time\temperature increases grain size and reduces porosity, there by decreases impediment to the domain wall motion. As a result the magnetization of ferrite increases with sintering time.

Part-B of chapter IV is devoted to the study of IR spectra of Co-Zn ferrites. In general, the IR spectra show

the presence of three to four bands. The high frequency band  $\nu_1$  (450 - 480  $\text{cm}^{-1}$ ) and low frequency band  $\nu_2$  (375-420  $\text{cm}^{-1}$ ) are assigned to tetrahedral and octahedral complexes respectively. A small band  $\nu_3$  (320-350  $\text{cm}^{-1}$ ) near  $\nu_2$  is assigned to octohedral metal-oxygen ion complexes. The lowest band  $\nu_4$  (290  $\text{cm}^{-1}$ ) for highest Cobalt concentration is attributed to lattice vibration of the system [15,16].

Ferrite mecrostructure is dealt with in detail in chapter V. Microstructure affects structure sensitive properties of the materials. These days it is possible for us to produce ceramic materials with desired properties, for specific applications, by controlling their microstructure by following appropriate sintering procedure during their manufacture.

In the present work SEM micrographs of samples  $\text{CoFe}_2\text{O}_4$  and  $\text{Co}_{0.6}\text{Zn}_{0.4}\text{Fe}_2\text{O}_4$  sintered at 900°C for 15 hrs and 30 hrs were obtained from the Mineralogical Institute, University of Mysore, Mysore. The average grain size of these samples was measured by the line intercept method [17] using travelling microscope. It is found that average grain size increases with increase in sintering time. The increase in grain size

increases densification, decreases porosity and hence increases conductivity and magnetization.

From the present study it can be concluded that porosity and grain size play an important role in deciding the activation energy, conduction mechanism and magnetization. Higher the sintering time more will be the conductivity, magnetization and less will be the activation energy for conduction in both para and ferrimagnetic regions. This is attributed to the increase in grain size and decrease in porosity at higher sintering time. However, it is essential to carry out the microstructural analysis of the samples over a wide range of sintering time and temperatures, for detailed understanding of microstructure-property correlation.

## REFERENCES

- [1] Jonker G.H.,  
J.Phys. Chem. Solids, 9 (1959), 165.
- [2] Josyulu O.S. and Sobhanadri J.,  
Phys. Status Solid A 59 (1980), 323.
- [3] Satyanarayana R, Ramana Murthy S, and Seshadri Rao T.,  
J.Less Common Metals, 86 (1982) 115 - 120.
- [4] Guillaud et al,  
in Standley's "Oxide Magnetic Materials", Oxford Univ.  
Press, (1962), 63.
- [5] Lavine B.F.,  
Phys. Rev. (USA), B-7, 259 (1973).
- [6] Standley K.J.,  
'Oxide Magnetic Materials", Oxford Univ. Press,(1962),25.
- [7] Bhuiya A.H., Rehaman J. and Paulit S.K.,  
Bangla Desh, J. of Scientific and Industrial Research,  
Vol.XV, No.1-4, P.116 (Jan-Oct, 1980).
- [8] Parker R.,  
"Magnetic Oxides", Part-I, Ed. Craik D.J.,  
John Wiley and Sons, P.422 (1975).
- [9] Irkhin In.P., and Turov E.A.,  
Fiz. Met. Metalloved, 4, P-9 (1957).
- [10] Parker R., and Tinsley C.J.,  
Ferrites, Proc. Int. Conf.Tokyo (1970), P.591.
- [11] Frohlich H.,  
Adv. Phys. 3 (1954), P.325.
- [12] Guillaud.,  
Magnetic properties of ferrites, J. Phys. Rad. 12,  
239 - 248 (1951).
- [13] Sinha A.P.B. and Menon P.G.,  
"Solid state Chemistry", Marcel Dekker, NY, P.385 (1974).
- [14] Sawant S.R., Patil S.A., and Patil R.N.,  
Indian J.Pure and Appl. Phys. Vol.19, (Dec,1981), P.1213.

- [15] Waldron R.D.,  
Phys. Rev. 99, 1727 (1955).
- [16] Preudhomme J. and Tarte P.,  
Spectrochem. Acta 27A, 1817 (1971).
- [17] Narayan R., Tripathi R.B., Das B.K. and Jain G.C.,  
"Microstructure and Grain growth Kinetics",  
J. Mat. Sci., 18, P. 1583 - 89 (1983).

...Oo\*oO...